

A MULTISLIT TRANSVERSE-EMITTANCE DIAGNOSTIC FOR SPACE-CHARGE-DOMINATED ELECTRON BEAMS

P. Piot, J. Song, R. Li, G.A. Krafft, D. Kehne, K. Jordan, E. Feldl, and J.-C. Denard,
Thomas Jefferson National Accelerator Facility, Newport News, VA 23606, *JUNA 17 1997*

Abstract

Jefferson Lab is developing a 10 MeV injector to provide an electron beam for a high-power free-electron laser (FEL). To characterize the transverse phase space of the space-charge-dominated beam produced by this injector, we designed an interceptive multislit emittance diagnostic. It incorporates an algorithm for phase-space reconstruction and subsequent calculation of the Twiss parameters and emittance for both transverse directions at an update rate exceeding 1 Hz, a speed that will facilitate the transverse-phase-space matching between the injector and the FEL's accelerator that is critical for proper operation. This paper describes issues pertaining to the diagnostic's design. It also discusses the acquisition system, as well as the software algorithm and its implementation in the FEL control system. First results obtained from testing this diagnostic in Jefferson Lab's Injector Test Stand are also included.

1 INTRODUCTION

Jefferson Lab is building a tunable high-power free-electron laser operating in the mid-infrared to study technologies required for high-average-power operation [1]. This FEL incorporates a 350 keV photocathode gun capable of generating a charge-per-bunch beam of typically 135 pC. After acceleration with two

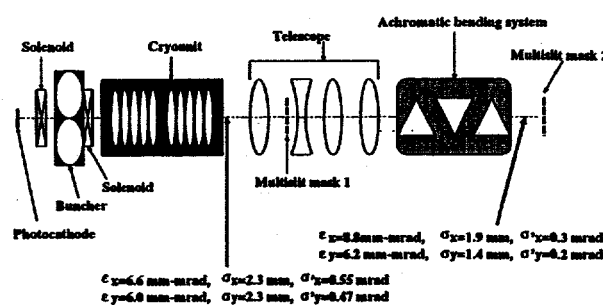


Figure 1: Schematic of the FEL injector. Normalized emittance, beam size and beam divergence at 135 pC bunch charge are given at the cryounit exit and the injection point according to PARMELA.

CEBAF five-cell superconducting cavities the beam is at 10 MeV and injected via an achromatic bending system into the driver linac that accelerates the electrons up to about 42 MeV prior to the wiggler interaction.

The transverse emittances at the wiggler location are required to be small (less than 13 mm-mrad) to operate the laser with a high gain and high extraction efficiency at full power. The specified transverse beam parameters at the wiggler constrain the emittance in the injector to be likewise small (Fig. 1). Therefore, in order to verify the emittance from the injector for operations, two multislit transverse-emittance diagnostics are going to be installed (Fig. 1) in the injector. A first monitor, located at the cryounit exit, will provide the necessary information to set the four matching quadrupoles of the downstream telescope. The second device allows beam parameters at the injection point in order to check the injector and linac are properly matched.

2 MULTISLIT TECHNIQUE

Techniques of phase-space sampling for emittance measurement are widely used for space-charge-dominated beams. The idea is to select one or several sample beamlets, at specific positions, by means of an intercepting mask in which small apertures have been machined. The beamlets retain the transverse temperature of the original beam at such low charge that space charge forces do not contribute significantly to the transverse momentum. The beamlets drift through a length long enough to allow the transverse momentum to impart a measurable contribution to the transverse position. The phase-space parameters can then be computed using the second-order moments ($\langle x^2 \rangle$, $\langle x'^2 \rangle$, $\langle xx' \rangle$) of the beamlet profiles [2]. There are several types of emittance monitors reported in the literature whose differences are essentially in the type of selecting apertures (pepper pot, slit,...) and the profile monitor used (wire-scanner, fluorescent screen,...). Among the different methods we choose to intercept the beam with a multislit mask [3,4] since it provides the fast and precise measurement we need during the commissioning and operation of our injector. The multislit assembly consists of a series of slits which collimate the space-charge-dominated incoming beam into the emittance-dominated beamlets that drift up to a profile monitor, an optical transition radiation (OTR) viewer in our case. The principal drawback of this diagnostic is its narrow emittance acceptance compared with other methods [5]. Therefore we optimized the slit design for a specific charge per bunch that we have chosen to be the full operating charge: 135 pC.

DISCLAIMER

This report was prepared as an account of work sponsored by an agency of the United States Government. Neither the United States Government nor any agency thereof, nor any of their employees, make any warranty, express or implied, or assumes any legal liability or responsibility for the accuracy, completeness, or usefulness of any information, apparatus, product, or process disclosed, or represents that its use would not infringe privately owned rights. Reference herein to any specific commercial product, process, or service by trade name, trademark, manufacturer, or otherwise does not necessarily constitute or imply its endorsement, recommendation, or favoring by the United States Government or any agency thereof. The views and opinions of authors expressed herein do not necessarily state or reflect those of the United States Government or any agency thereof.

DISCLAIMER

**Portions of this document may be illegible
in electronic image products. Images are
produced from the best available original
document.**

3 DESIGN CONSIDERATION

3.1 Analytic Conditions

Due to mechanical constraints, a drift distance (L) was chosen to be 620 mm. The choice of the geometric parameters (slit width w and spacing d) are then imposed by three conditions.

(i) The beamlets must be emittance-dominated since space-charge expansion would cause appreciable broadening of the angular spread over the drift. We calculate the space-charge-over-emittance ratio defined from the transverse K-V equation to be about $R \simeq 11.75$ using the beam parameters predicted with PARMELA. After the multislit mask the value of the ratio, R' , for one beamlet is scaled accordingly to: $R' = R/12 \times (w/\sigma)^2$, σ being the rms beam size. Setting w to 100 μm yields a ratio $R' = 2.8 \times 10^{-3}$. This guarantees the space-charge force contribution to transverse momentum is insignificant.

(ii) The beamlet profiles must not overlap on the screen, which implies the drift length (L) and the inter-slits distance (d) are related by: $4\sigma'L < d$. σ' is the rms beam divergence.

(iii) Finally, the resolution in position and in divergence should be comparable, i.e. $\sigma/d = L\sigma'/\rho$, where ρ is the resolution of the detector.

The two latter conditions yield a slits spacing of about 1.1 mm. The values determined for w and d have been used as a starting point for accurate numerical simulation of the slits with PARMELA.

3.2 Optimization with Numerical Simulations

We developed a MATLAB-based program to retrieve the phase-space parameters and distribution from a simulated OTR image. The image is generated from the distribution predicted by PARMELA, retracing each electron from before the slits up to the OTR screen. We optimized the design, after many iterative runs, changing the slit width and spacing, to try to minimize the error in the retrieved parameters over the required emittance range (normalized rms emittance between 4 and 20 mm-mrad). The values we finally found reasonable are: $w=75 \mu\text{m}$ and $d=1.5 \text{ mm}$. According to our simulation results for different emittances (by scaling the nominal one) we are confident in achieving a relative error on emittance and Twiss parameters of the order of 10%. Table 1 compares the nominal emittance with the one computed from the beamlet's OTR image.

3.3 Some Mechanical Considerations

In order to avoid using any cooling system, we have opted to make the slits out of copper and have a thermal bridge that quickly dissipates the heat toward the exterior of the vacuum chamber. In order to reduce the deposited power below the damage threshold of

$\epsilon_{\text{PARMELA}}$ (mm-mrad)	$\epsilon_{\text{RETRIEVED}}$ (mm-mrad)
8.094	8.077
3.947	4.014
24.282	23.016

Table 1: Typical retrieved value for the normalized emittance obtained simulating the multislit mask using a phase-space distribution predicted by PARMELA

3 W we will use a low duty factor beam mode for emittance measurement, which is possible since the physics of our beam is only dominated by single-bunch effects (bunch spacing is 8.02 m). The multislit mask thickness is a compromise between noise and angular acceptance: if the mask is not thick enough, electrons that go through copper can contribute to the OTR pattern. On the other hand, increasing the thickness would imply more stringent tolerance on the slit alignment with respect to the beam axis. After estimating multiple scattering, which is the dominant process for 10 MeV electrons, we set the thickness to 5 mm, which yields an angular acceptance of approximately 10 mrad. For this angle 10% of the electrons are lost because of edge scattering. The final design of the multislit assembly has two sets of thirteen slits that allow x and y transverse-emittance measurement. When the slits are removed from the beam path, a high-frequency shield insures beam-pipe continuity to minimize the wakefield impedance.

4 CONTROL AND ACQUISITION SYSTEM

The beamlet's OTR pattern is monitored with a charge-coupled-device camera whose analog video signal is digitized and processed using a DATACUBE VME-based frame grabber operating with its own VME input-output controller (IOC). In addition to digitizing, the CPU of the video board performs elementary image-processing functions such as background subtraction, projection along an axis, etc. The output of the DATACUBE, in our case a projection that contains the beamlet profiles, is transferred to the IOC on which we have implemented VxWorks routines. After identifying each beamlet profile and the slit it comes from, the code computes the emittance and Twiss parameters. The results can then be accessed from any X-station via the EPICS channel-access protocol. We developed X-window based screens that display emittance, Twiss parameters and possibly phase-space isocontours. The achieved speeds are, respectively, about 1 and 2 sec for updating parameters and plot refresh, a speed that allows observing the phase space parameters in real time while tuning the injector. Storing raw data and pro-

jections is also possible at each stage of the process for more detailed off-line analysis, e.g. using (time and CPU consuming) powerful image processing tools.

5 FIRST RESULTS

Since the 10 MeV energy region of the injector was not yet available, we chose to conduct the preliminary tests on the Jefferson Lab Injector Test Stand at 250 keV. The configuration is similar to that described elsewhere [5], consisting of a photocathode gun, a solenoid, and a diagnostic beamline. The charge-per-bunch was set to approximately 5 pC so that the achieved emittance is within the multislit assembly acceptance. Also, because of the low energy, we had to use a fluorescent viewer instead of an OTR viewer.

On Figure 2 we present an example beamlet profile. Depending on the solenoid setup, we were able to illuminate up to 8 slits, a very good number for emittance measurement with a 10% level accuracy. Unfortunately, we were not able to perform our measurement with such high number of peaks because of the reduced available area on the fluorescent viewer. Several

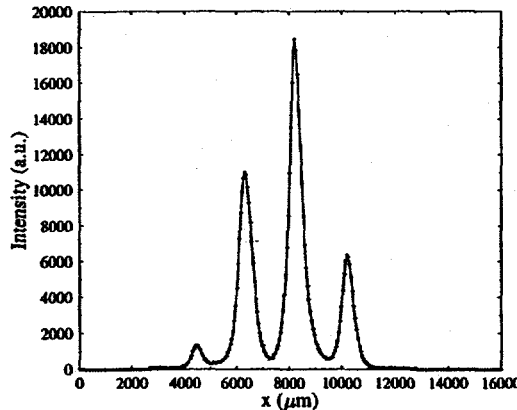


Figure 2: Typical beamlet profile obtained on a fluorescent screen at 250 keV with a charge-per-bunch of 5 pC.

cross-checks have been made with the single-slit-wire emittance diagnostic used in Reference [5] and both methods agreed within 10-15% for the emittance and the β -function. However, there is still substantial disagreement concerning the α -parameter, probably due to a not precise enough scale calibration of our fluorescent screen. This problem should be solved on the final version of the diagnostic where we plan to have precise calibration lines on the OTR screen.

We also measured the emittance versus the charge per bunch, for two macropulse width, as depicted in Figure 3, keeping the solenoid field value constant. The discrepancies between the two sets of data at low charge are probably due to low charge ghost pulses that are created as a consequence of laser light leaks between two consecutive micropulses. Therefore the

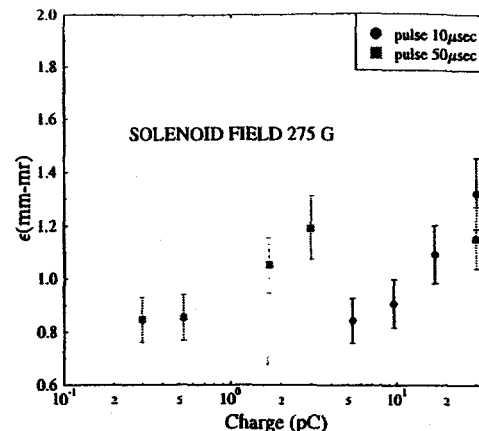


Figure 3: Unnormalized emittance versus charge for two different macropulse widths. Error bars of 15% have been considered after comparison with the single-slit-wire method.

wider the macropulse, the larger the ghost pulse contribution to emittance is.

Further studies and quantitative comparison of the multislit mask, with the single-slit-wire technique in the Injector Test Stand and with the one-quadrupole-OTR method in the FEL injector, will be forthcoming.

6 ACKNOWLEDGMENTS

The authors would like to thank S. Benson, C. L. Bohn, and G. Neil for useful discussions, and H. Liu and B. Yunn for their help with PARMELA. We are indebted to R. Legg and M. Shinn for setting up the beam during our experiment. This work was funded by the U.S. DOE contract DE-AC05-84ER-401 and the Office of Naval Research.

7 REFERENCES

- [1] C. L. Bohn, "Recirculating Accelerator Driver for a High-Power Free-Electron-Laser: A Design Overview", these proceedings.
- [2] P. Lapostolle, "Quelques effets essentiels de la charge d'espace dans les faisceaux continus", Rep. CERN/DI-70-36 (1970).
- [3] S. C. Hartman, "The UCLA High-Brightness RF Photo-Injector", PhD thesis, University of California, Los Angeles (unpublished) and J. Rosenzweig and G. Travish, "Design Considerations for the UCLA PBPL Slit-Based Phase Space Measurement Systems", PBPL Internal (Feb 1994).
- [4] M. Crescenti, U. Raich, "A Single Pulse Beam Emittance Measurement for the CERN Heavy Ion Linac", U. Raich, private communication.
- [5] D. Engwall et al., "A High-Voltage-DC GaAs Photoemission Gun: Transverse Emittance and Momentum Spread Measurement", these proceedings.